Applied Energy 212 (2018) 1462–1475

Contents lists available at ScienceDirect

Applied Energy

journal homepage: www.elsevier.com/locate/apenergy

Interactive game vector: A stochastic operation-based pricing mechanism for smart energy systems with coupled-microgrids

Tianguang Lu[a,*], Qian Ai[a], Zhaoyu Wang[b]

[a] Shanghai Jiao Tong University, Shanghai 200240, China
[b] Iowa State University, Ames, IA 50011, USA

HIGHLIGHTS

- A dynamic pricing mechanism is proposed for smart energy systems considering operation quality.
- An informative game vector is established to perform price-based energy interactions among MGs.
- A stochastic method is integrated into the proposed method to handle the renewable uncertainty.
- Comprehensive results and analysis in dynamic energy market environment are provided.

ARTICLE INFO

Keywords:
Microgrid
Game vector
Stochastic programming
Bi-level programming
Smart energy system
Dynamic market operation

ABSTRACT

To accommodate the large scale of renewable energy resources now widely integrated into power systems, an interactive two-level pricing mechanism for coupled microgrids (MG) in a smart energy system is proposed that considers operational quality and renewable generation uncertainty. In the upper level of the pricing mechanism, the distribution energy market operator (DEMO) guarantees operational quality by trading energy with coupled microgrids, while the actual transactions between networked microgrids is performed at the lower level. Stochastic programming is applied to handle the uncertainty caused by large-scale renewable integration. An innovative time-varying game vector and energy transaction strategy deal with the spatio-temporal market interaction of the networked microgrids, where each microgrid is able to directly trade all types of energy with any other microgrid at any time. The proposed model is solved using a customized hierarchical genetic algorithm. Case studies on an IEEE bus test feeder and an existing energy system in China demonstrate the effectiveness of the proposed methodology.

1. Introduction

In recent years, large-scale renewable energy resources have been widely integrated into power systems [1]. Microgrids (MG) are localized grids that can include a smart cluster of energy storage systems (ESS), distributed generators (DG), and flexible consumer loads [2,3], and are believed to be a promising paradigm that can facilitate renewable utilization and regional energy regulation [4]. As a result, there is growing interest in adopting multiple MGs in a smart energy system to further enhance system reliability, operations, environmental friendliness, and economic benefits under large-scale renewable integration. However, to ensure the stability, reliability, and economic profit of MGs, new market mechanisms are needed to coordinate the interaction between MGs and the wider power system, and deal with the highly variable nature of renewable generation and load consumption [5].

Optimal pricing mechanisms for MGs in retail energy markets have been extensively studied in the literature. In [6], a day-ahead electricity pricing strategy was proposed under arbitrary utility and cost structures. The system model could accommodate heterogeneous user requirements and constraints in a generalized problem formulation to maximize the profits of the entities involved. Ref. [7] developed a nonlinear and randomized pricing mechanism for a demand response-enabled MG to perform distributed management of flexible loads. The flexibility restriction imposed by a previously proposed measure was replaced by a soft nonlinear price signal to produce more efficient resource management. The work in [8] introduced real time pricing and combined power scheduling of electric appliances in a residential energy management system that considered the reduction of peak power to average ratio over a large number of end consumers. The introduced pricing scheme of a smart house minimized the consumption cost.

* Corresponding author.
E-mail addresses: ltghaoo@163.com (T. Lu), aiqian@sjtu.edu.cn (Q. Ai), wzy@iastate.edu (Z. Wang).

https://doi.org/10.1016/j.apenergy.2017.12.096
Received 30 September 2017; Received in revised form 6 December 2017; Accepted 27 December 2017

Nomenclature

Indices and sets

t	time index $t \in T$
s	scenario index $s \in \mathscr{S}$
I	set of microgrid (MG)/point of common coupling (PCC) nodes
O	set of MGs that linked to MG i
F/M_i	set of nodes in distribution network/MG i

Parameters

C^{loss}	unit cost of power loss
C^{sel}	sell price of the exchange power from MGs to the distribution energy market operator (DEMO)
C^{buy}	purchase price of the exchange power from the DEMO to MGs
C^{G}	generation cost of the distributed generator (DG) in the distribution network
R_t	spare capacity
x_f/r_f	resistance/reactance of line f-$f+1$
$C^{\text{SBRE}}_{f,t}$	dynamic trade price of $P^{\text{SBRE}}_{f,t}$
$C^{\text{rin}}_{f,t}$	dynamic trade price of $P^{\text{rin}}_{f,t}$
$C^{\text{SBIN}}_{f,t}$	dynamic trade price of $P^{\text{SBIN}}_{f,t}$
$C^{\text{SBLE}}_{f,t}$	dynamic trade price of $P^{\text{SBLE}}_{f,t}$
$C^{\text{rout}}_{f,t}$	dynamic trade price of $P^{\text{rout}}_{f,t}$
$C^{\text{SBOUT}}_{f,t}$	dynamic trade price of $P^{\text{SBOUT}}_{f,t}$
C^{MT}	unit cost of microturbine (MT) generation
$C^{\text{ERE}}/C^{\text{ELE}}$	unit cost/profit of rented capacities
$P^{\text{rs}}_{f,t}$	renewable generation of MG i at node f in scenario s
$R^{\text{up}}_{\text{MT}}/R^{\text{down}}_{\text{MT}}$	ramp rates of a MT
η/μ	output thresholds of $E^{\text{SBLE}}_{f,t}/E^{\text{SBRE}}_{f,t}$
$\Delta C^{k}_{i,t}$	dynamic makeup price of the k^{th} category of tradable energy and service in MG i
$P_{f,t}/Q_{f,t}$	active/reactive power flow from node f to $f+1$

Variables

$V_{f,t}$	voltage at node i
$P^{\text{MT}}_{f,t}$	MT generation at node f
$P^{\text{SBRE}}_{f,t}$	the energy of MG i at node f in other energy storage systems (ESS)
$P^{\text{rin}}_{f,t}$	traded renewable generation from other MGs to MG i at node f
$P^{\text{SBIN}}_{f,t}$	traded ESS generation from other MGs to MG i at node f
$P^{\text{SBLE}}_{f,t}$	energy of other MGs in MG i's ESS at node f
$P^{\text{rout}}_{f,t}$	traded renewable generation from MG i to other MGs at node f
$P^{\text{SBOUT}}_{f,t}$	traded ESS generation from MG i to other MGs at node f
$E^{\text{SBRE}}_{f,t}$	MG i's cumulative rented capacity of other MGs at node f until time t
$E^{\text{SBLE}}_{f,t}$	other MGs' cumulative rented capacity of MG i at node f until time t
$P^{\text{SB}}_{f,t}$	storage battery (SB) output at node f
$P^{L}_{f,t}/Q^{L}_{f,t}$	active/reactive load at node f
$P^{\text{TL}}_{f,t}/Q^{\text{TL}}_{f,t}$	total active/reactive power exchange between MG i and the DEMO at bus f

Aghajani et al. [9] presented a scheduling model for pricing demand response rate in microgrid energy management, with multi-objective dispatch, demand response providers, and price-offer packages used to optimize operations and reduce emission costs.

Most existing pricing mechanisms are based on bidding between a single MG and the wholesale energy market without considering any interactions between different MGs. Although the coordinated energy management of networked MGs with energy sharing has been widely discussed in the literature [10,11], the price response characteristics are based on assumed mathematical functions, where a certain price leads to a specific energy consumption level. These functions cannot mimic the realistic dynamic pricing decision-making of each MG. While some studies in [12,13] concerning auction strategies were based on multi-agents, the developed functions could not directly perform multiple transactions with any agent at any time. Moreover, the underlying distribution network is neglected in most of the existing literature. The MGs, if not operated in an islanded mode, are connected to the main grid via the power control center (PCC) [14]. For this reason, the associated power flow constraints and other system operational constraints of the distribution networks should be taken into account, such that the obtained scheme can be applicable to actual systems with guaranteed stability and reliability [15,16].

With the rapid development of integrated energy systems, the transaction of different types of energy has drawn considerable attention in recent energy system research. Ref. [17] proposed an analytical framework that studied East Asian gas markets, where the distinctive economics were used to assess policy options to address market failures. A region characterized by a high density of energy-intensive processes was used in [18] to find the economic potential in connecting three industrial plants and four energy companies within three local district heating systems to a regional heat market in which different operators provided heat to a joint district heating grid. To investigate the possibility of using district heating and cooling systems (DHC) for capacity market auctions, the authors in [19] developed two models for operating a DHC system: electricity-adjustment capacity provision and electricity-adjustment operation. In particular, the two models were solved using particle swarm optimization to reduce computational cost. The impact of different support schemes on the retail price of micro-combined heat and power units based on solid oxide fuel cells was analyzed in [20] in the residential sector, where the implications of each incentive toward the technical implementation of the technology were also analyzed. Despite these efforts, most works have only considered transactions concerning a single type of energy. Although some forms of integrated energy systems have been developed in some market studies, the trade mechanism was not fully detailed.

Considering the stochastic nature of renewable generation and user consumption, stochastic programming has also been intensively studied for both MGs and bulk energy systems [21]. Ref. [22] proposed a stochastic resource scheduling model for a grid-connected MG. A stochastic problem was formulated to minimize both the expected operational cost of the MG and power losses while accommodating the intermittent nature of the renewable energy resources. In [23], a Bender's decomposition algorithm was presented to reduce the computational burden of stochastically programming a MG with high photovoltaic (PV) power generation. The study in [21] presented a stochastic operational scheme for a MG with greenhouse gas emissions. Two different stochastic approaches based on sample average approximation and probabilistic constrained stochastic programming were formulated to cooptimize carbon emissions and power generation fuel costs while mitigating the impact of the intermittence of the renewable energy generated. However, most of the studies mentioned here were conducted to optimize the power generation fuel cost of a single MG.

That being said, limited stochastic studies have been performed to consider the complex and interactive impact of coupled MGs in a smart energy system [24].

Game theory is a promising approach to dealing with the interaction of coupled MGs [25], where each MG is taken as an independent entity concerned with making purchases to maximize its own profit. There are primarily two categories of game theory-based market interaction. The first category is based on the one-step process, which is aimed at making optimal strategies and adjusting power usage during certain time periods [26,27]. The second category is based on a dynamic decision process that considers time-variant gaming, where the final optimum is obtained through iterative market interactions [28,29]. To obtain a unique Nash equilibrium, most literature has simplified their market strategy game models and limited the information a game should have, which means the models cannot accommodate good market interactions among smart energy systems.

To solve the above-mentioned limitations, this paper designs an innovative two-level pricing mechanism to coordinate MG interactions through a proposed dynamic game-vector decision making method. In the upper level of the mechanism, the distribution energy market operator (DEMO) secures operational quality and bids with the MGs. In the lower level, each MG bids for use of its multiple energy resources with the DEMO and other MGs. The key to the proposed mechanism is using game vectors to mimic the spatio-temporal market pricing behavior of each MG, which can directly bid its energy and storage service against any other MG at any time. The stochastic programming is integrated into the pricing model to consider the prediction error of the intermittent renewable generation. The proposed model is solved through a customized hierarchical genetic algorithm (C-HGA).

The main contributions of this paper are:

1. An interactive pricing mechanism is proposed for smart energy systems with coupled MGs that considers operational quality.
2. An informative game vector is established to model the spatio-temporal market interactions of coupled MGs, where each MG is able to directly trade all types of its energy production and services with any other MG at any time.
3. A dynamic-rolling priority-based bidding and settlement strategy is proposed based on a newly-defined platform of tradable energies and storage services.
4. A stochastic method is integrated into the proposed pricing mechanism to deal with the uncertainty caused by intermittent renewable generation.
5. Comprehensive results and analyses in dynamic energy market environments are provided.

The rest of this paper is organized as follows. Section 2 introduces the proposed pricing mechanism framework. The upper-level model is presented in Sections 3 and 4 illustrates the lower-level model with stochastic programming. The proposed dynamic game vector-based trade mechanism is presented in Section 5. The C-HGA is implemented in Section 6. Section 7 analyzes the numerical results, followed by the conclusion in Section 8.

2. Pricing mechanism framework

2.1. Distribution system structure

For this work, a smart energy system is managed by a DEMO and contains multiple MGs, controllable DGs, and static volt-ampere reactive (VAR) compensations (SVCs). The DEMO, as an entity, maintains system operational quality by trading energy with MGs and regulating the grid-connected DGs and SVCs. Each MG includes loads, renewable (wind turbines and PVs) and controllable (microturbines) DGs, and its energy storage system (storage batteries). As a part of the distribution network, each MG trades its energy or service through an aggregator energy exchange network (AEEN) at the point of common coupling (PCC). An AEEN is the part of a distribution systems that allows a pricing mechanism to be applied to enable power exchange among MGs. That is, different MGs can exchange power through the distribution network's AEEN [30]. Fig. 1 shows the structure of an interaction-enabled distribution system.

2.2. Energy and storage service on transaction

With the introduction of an AEEN, each MG is capable of offering tradable energy and storage service, which come from the following three sources. The first source is its renewable power generation. The second source is the energy stored in each MG's ESS. The third source comes from the available storage capacity in other MGs' ESSs as well as the energy stored in their ESSs.

2.3. Two-level pricing framework

In Fig. 2, the pricing mechanism is formulated as a two-level optimization model. The upper level optimizes the operational quality through interactions among the DEMO, MGs, and grid-connected devices. The lower level optimizes each MG's profit and coordinates energy interactions among MGs. The exchanging variable between the upper and lower levels is $P_{f,t}^{\mathrm{TL}}$.

The proposed pricing mechanism is applied by the microgrids to perform the market interaction among networked microgrids. The microgrids trade their energy and storage service with each other based on the proposed pricing mechanism to increase their profit. The market operator supervises the market behavior of the microgrids and maintains the system operation quality according to the proposed mechanism.

3. Upper-level problem formulation

3.1. Distribution network model

Consider a radial network as shown in Fig. 3, with n buses indexed by $f = 0,1,...,F$. DistFlow [31] equations can be used to describe the

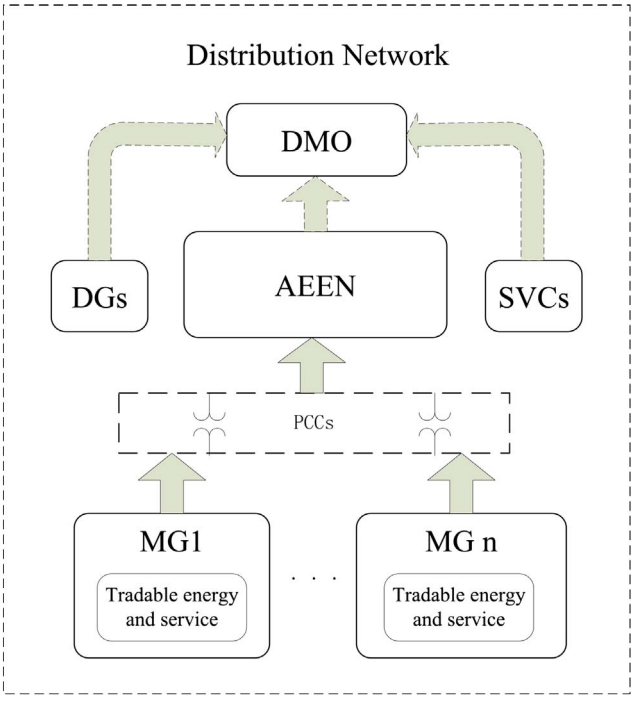

Fig. 1. Distribution system structure.

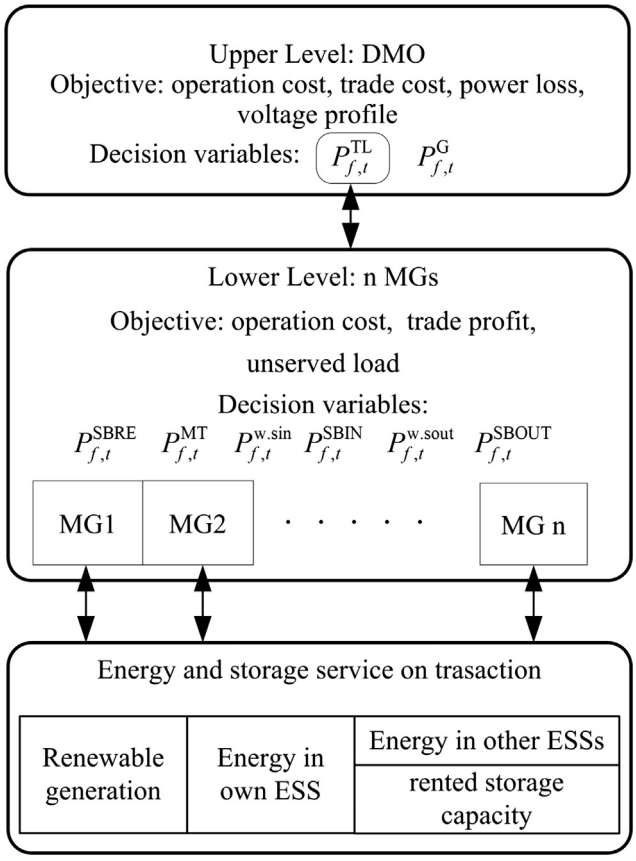

Fig. 2. Pricing mechanism framework.

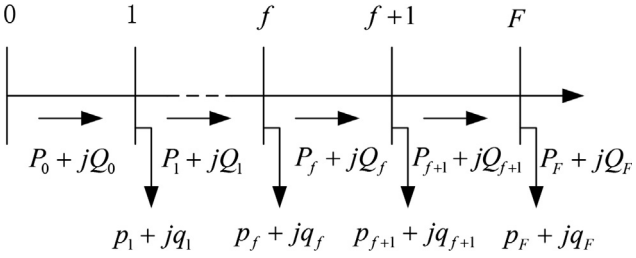

Fig. 3. Distribution network structure.

complex power flows at each node f. The DistFlow equations can be simplified using linearization in (1) for $\forall\, t,f \in F$. The linearized power flow equations have been extensively used and justified in both traditional distribution systems and MGs [32–34]. Thus, we can write

$$\begin{cases} P_{f+1,t} = P_{f,t} + p_{f+1,t} \\ Q_{f+1,t} = Q_{f,t} + q_{f+1,t} \\ V_{f+1,t} = V_{f,t} + (r_f P_{f,t} + x_f Q_{f,t})/V^2_{f,t} \\ p_{f,t} = P^{L}_{f,t} - P^{G}_{f,t} \\ q_{f,t} = Q^{L}_{f,t} - Q^{G}_{f,t} \end{cases} \tag{1}$$

where P^{G}_{f} and Q^{G}_{f} denote node injections from microturbines, SVCs, and renewable generators.

3.2. Upper-level model

The optimization problem of the DEMO strategy model can be described as

$$\begin{aligned} \min F = & \sum_{t=1}^{T} C^{loss} P^{loss}_{t} + \\ & \sum_{t=1}^{T} \sum_{f \in I} [C^{sel}(|P^{TL}_{f,t}| - P^{TL}_{f,t})/2 - C^{buy}(|P^{TL}_{f,t}| + P^{TL}_{f,t})/2] + \\ & \sum_{t=1}^{T} \sum_{f \in F} C^{G} P^{G}_{f,t} + \\ & \mu \sum_{t=1}^{T} \sqrt{\sum_{f \in F} (V_{f,t} - 1)^2 / F} \end{aligned} \tag{2}$$

where the first item is the cost of the network power loss, the second item denotes the cost of trading power energy between the DEMO and its MGs, the third item represents the operational cost of the grid-connected device generation, and the fourth item indicates the level of voltage deviations at all nodes of the distribution network with a penalty factor μ to unify the unit. The upper-level model stands for the distribution-level operation. Therefore, its operation cost comes from the DGs and SVCs that are connected to the distribution network.

Constraints on outputs, voltages, line capacity, and the spare capacity of the distribution network are shown in (3)–(5). Constraint (6) describes that the total generation should be equal to or larger than the total load.

$$\begin{cases} P^{G}_{f,t} - P^{G}_{f,t-1} \leqslant R^{up} \\ P^{G}_{f,t-1} - P^{G}_{f,t} \leqslant R^{down} \end{cases} \tag{3}$$

$$\begin{cases} \underline{P^{TL}} \leqslant P^{TL}_{f,t} \leqslant \overline{P^{TL}} \\ \underline{Q^{TL}} \leqslant Q^{TL}_{f,t} \leqslant \overline{Q^{TL}} \\ \underline{P^{G}} \leqslant P^{G}_{f,t} \leqslant \overline{P^{G}} \\ \underline{P^{G}} \leqslant P^{G}_{f,t} \leqslant \overline{P^{G}} \\ \underline{P_f} \leqslant P_{f,t} \leqslant \overline{P_f} \end{cases} \tag{4}$$

$$\sum_{f \in F} (\overline{P^{G}} - P^{G}_{f,t}) \geqslant R_t \tag{5}$$

$$\sum_{f \in F} (P^{G}_{f,t} - P^{L}_{f,t}) + \sum_{f \in I} P^{TL}_{f,t} \geqslant 0 \tag{6}$$

4. Lower-level problem formulation

4.1. The first-stage stochastic problem

The lower-level model is an n-follower optimization. The deterministic cost of MG i resulting from competing with other MGs and the DEMO is composed of two parts: the operational cost of MTs and the cost of trading energy and service. For $\forall\, t,i \in I$, the formulation to minimize cost is

$$\begin{aligned} \min f_i = & \sum_{t=1}^{T} \sum_{f \in M_i} ((C^{MT} P^{MT}_{f,t} \\ & + C^{SBRE}_{f,t} P^{SBRE}_{f,t} + C^{rin}_{f,t} P^{rin}_{f,t} + C^{SBIN}_{f,t} P^{SBIN}_{f,t} \\ & - (C^{SBLE}_{f,t} P^{SBLE}_{f,t} + C^{rout}_{f,t} P^{rout}_{f,t} + C^{SBOUT}_{f,t} P^{SBOUT}_{f,t}) \\ & + (C^{ERE} E^{SBRE}_{f,t} - C^{ELE} E^{SBLE}_{f,t}) \\ & - (C^{sel}(|P^{TL}_{f,t}| - P^{TL}_{f,t})/2 - C^{buy}(|P^{TL}_{f,t}| + P^{TL}_{f,t})/2))) \\ & + \mathcal{Q}(p) \end{aligned} \tag{7}$$

where

$$\mathcal{Q}(p) = \mathbb{E}_s \phi(p,s) = \sum_{s \in \mathcal{S}} Pr(s) \phi(p,s) \tag{8}$$

The above objective function (7) includes the first-stage cost and the second-stage expected cost. For the purpose of illustration, the decision

variables $P_{f,t}^{\mathrm{SBRE}}$,$P_{f,t}^{\mathrm{rin}}$,$P_{f,t}^{\mathrm{SBIN}}$,$P_{f,t}^{\mathrm{SBLE}}$,$P_{f,t}^{\mathrm{rout}}$, and $P_{f,t}^{\mathrm{SBOUT}}$ will be described in Section 5. In (8), $Pr(s)$ indicates the probability of realization for $s \in \mathscr{S}$, and $\mathbb{E}_s$ is defined as the expectation with respect to $\mathscr{S}$. If $P_{f,t}^{\mathrm{SBRE}}$ is positive, then the stored energy is discharged to supply MG i; otherwise, the extra energy is stored in the rented ESS capacity in other MGs. If $P_{f,t}^{\mathrm{SBLE}}$ is positive, then the stored energy of MG i is discharged to supply other MGs; otherwise the extra energy is stored in the rented capacity of the ESS in MG i.

The objective function (7) is subject to the following constraints (for $\forall\, t,i \in I$).

Energy generation limits:

$$\begin{cases} \underline{P^{\mathrm{MT}}} \leqslant P_{f,t}^{\mathrm{MT}} \leqslant \overline{P^{\mathrm{MT}}} \\ -\overline{P^{\mathrm{SB}}} \leqslant P_{f,t}^{\mathrm{SB}} + P_{f,t}^{\mathrm{SBLE}} + P_{f,t}^{\mathrm{SBOUT}} \leqslant \overline{P^{\mathrm{SB}}} \end{cases} \tag{9}$$

where the max and min superscripts denote the maximum and minimum outputs of the MT and EES.

Ramp rate constraints of the MT:

$$\begin{cases} P_{f,t}^{\mathrm{MT}} - P_{f,t-1}^{\mathrm{MT}} \leqslant R_{\mathrm{MT}}^{\mathrm{up}} \\ P_{f,t-1}^{\mathrm{MT}} - P_{f,t}^{\mathrm{MT}} \leqslant R_{\mathrm{MT}}^{\mathrm{down}} \end{cases} \tag{10}$$

Capacity constraints of the storage battery (SB) ESS:

$$\begin{cases} E_{f,t} = E_{f,t-1} - (P_{f,t}^{\mathrm{SB}} + P_{f,t}^{\mathrm{SBLE}} + P_{f,t}^{\mathrm{SBOUT}}) \\ \underline{E} \leqslant E_{f,t} \leqslant \overline{E} \\ E_{f,t}^{\mathrm{SBLE}} = E_{f,t-1}^{\mathrm{SBLE}} - P_{f,t}^{\mathrm{SBLE}} \\ E_{f,t}^{\mathrm{SBRE}} = E_{f,t-1}^{\mathrm{SBRE}} - P_{f,t}^{\mathrm{SBRE}} \\ 0 \leqslant E_{f,t}^{\mathrm{SBLE}} \leqslant \eta\overline{E} \\ 0 \leqslant E_{f,t}^{\mathrm{SBRE}} \leqslant \mu\overline{E} \end{cases} \tag{11}$$

Note that, for simplicity, this paper ignores charge/discharge efficiency factors.

4.2. The second-stage stochastic problem

The second-stage problem is established after the first stage is determined (for $\forall\, t,i \in I,s \in \mathscr{S}$)

$$\phi(p,s) = \min \sum_{t=1}^{T} \gamma_t \psi_t^s(\Delta p_{i,t}^s) \tag{12}$$

$$\begin{cases} \psi_t^s = \max\{0, \Delta p_{f,t}^s\} \\ \Delta p_{i,t}^s = \sum\limits_{f \in M_i} (P_{f,t}^{\mathrm{L}} - P_{f,t}^{\mathrm{MT}} - P_{f,t}^{\mathrm{SB}} - P_{f,t}^{\mathrm{TL}} - P_{f,t}^{\mathrm{r},s}) \end{cases} \tag{13}$$

The objective function (12) minimizes the penalty cost of the unserved load $\Delta p_{i,t}^s$ caused by the stochastic nature of renewable energy generation [35].

The objective function is subject to the following constraints:

$$0 \leqslant P_{f,t}^{\mathrm{rout}} + P_{f,t}^{\mathrm{rin}} \leqslant P_{f,t}^{\mathrm{r},s} \tag{14}$$

$$a_{i,t}^1 = \begin{cases} 1 & \sum\limits_{f \in M_i} (P_{f,t}^{\mathrm{L}} + P_{f,t}^{\mathrm{SB}} - P_{f,t}^{\mathrm{r},s}) < 0 \\ 0 & \sum\limits_{f \in M_i} (P_{f,t}^{\mathrm{L}} + P_{f,t}^{\mathrm{SB}} - P_{f,t}^{\mathrm{r},s}) \geqslant 0 \end{cases} \tag{15}$$

$$a_{i,t}^2 = \begin{cases} 1 & \sum\limits_{f \in M_i} (P_{f,t}^{\mathrm{L}} - P_{f,t}^{\mathrm{r},s}) > 0 \\ 0 & \sum\limits_{f \in M_i} (P_{f,t}^{\mathrm{L}} - P_{f,t}^{\mathrm{r},s}) \leqslant 0 \end{cases} \tag{16}$$

$$a_{i,t}^3 = \begin{cases} 1 & P_{f,t}^{\mathrm{L}} - P_{f,t}^{\mathrm{MT}} - P_{f,t}^{\mathrm{SB}} - P_{f,t}^{\mathrm{r},s} > 0 \\ 0 & P_{f,t}^{\mathrm{L}} - P_{f,t}^{\mathrm{MT}} - P_{f,t}^{\mathrm{SB}} - P_{f,t}^{\mathrm{r},s} \leqslant 0 \end{cases} \tag{17}$$

where constraint (14) denotes the limit of the renewable generation that MG i can sell to other MGs. Constraints (15)–(17) represent binary condition variables, which will be further described in Section 5.

Due to the continuity of the probability distributions, it is difficult to analytically address uncertainties. To handle this difficulty, the sample average approximation (SAA) method is applied to generate a certain number of scenarios to represent the probability distribution of the random parameters [21]. Therefore, (13) can be replaced by its approximate form

$$\mathscr{Q}(p) = \frac{1}{S} \sum_{s \in \mathscr{S}} \sum_{t=1}^{T} \gamma_t \psi_t^s(\Delta p_{i,t}^s) \tag{18}$$

where the scenario set has S realizations of random variable $P_{f,t}^{\mathrm{r},s}$. Studies have proved that the optimal solution of the reformulated two-stage stochastic problem will converge to the original solution if a sufficient number of scenarios are performed [36]. Hence, the original stochastic problem is reformulated as a continuous deterministic optimization problem.

5. Trade decision and game vector

5.1. Trade mechanism

A dynamic trade mechanism is established that truly represents the market behavior of interactive MGs. To define the decision objects for a specific type of energy or service, MGs are classified into demanders and suppliers and placed in the need pool (NP) and supply pool (SP), respectively. In addition, binary condition variables are introduced to model the market behavior. If a specific condition is satisfied, the variable is set to 1. If the SP condition variable is 1 for a MG, then the MG belongs to the SP; if the NP condition variable is 1, then the MG belongs to the NP. In (15) and (16), $a_{i,t}^1$,$a_{i,t}^2$, and $a_{i,t}^3$ are binary condition variables of the decision variables $P_{f,t}^{\mathrm{SBRE}}$,$P_{f,t}^{\mathrm{rin}}$, and $P_{f,t}^{\mathrm{SBIN}}$, respectively. When the binary variable is set to 1, its corresponding decision variable belongs to the NP; when the binary variable is set to 0, its corresponding decision variable is out of the NP. Due to complementarity, the binary condition variables of the SP are $1-a_{i,t}^1$,$1-a_{i,t}^2$, and $1-a_{i,t}^3$.

After classification of the NP and SP, each MG in the NP has a dynamic makeup $\Delta C_{i,t}^k$ with respect to t. At time t, MGs with higher $\Delta C_{i,t}^k$ have a higher priority to purchase any available tradable energy and service from MGs in the SP when multiple MGs are bidding together. During the bidding, MGs in the SP, which post a lower price including a demander's makeup, have the higher priority to offer the demander the tradable energy or service. In addition, the determination of the value of $\Delta C_{i,t}^k$ can be based on several approaches. In this paper, we assume that each MG cannot access the pricing information of other MGs. Hence $\Delta C_{i,t}^k$ is determined by the demand degree of MG i at t, i.e., $P_{i,t}^{\mathrm{D}} = \sum_{f \in M_i} (P_{f,t}^{\mathrm{L}} - P_{f,t}^{\mathrm{MT}} - P_{f,t}^{\mathrm{SB}} - P_{f,t}^{\mathrm{r},s})$. At each period of time, $\Delta C_{i,t}^k$ is standardized from $\underline{\Delta C_i^k}$ to $\overline{\Delta C_i^k}$ according to $P_{i,t}^{\mathrm{D}}$, where

$$\Delta C_{i,t}^k = \underline{\Delta C_i^k} + (\underline{\Delta C_i^k} - \overline{\Delta C_i^k}) P_{i,t}^{\mathrm{D}} / \max\{P_{i,t}^{\mathrm{D}} | t \in T\} \tag{19}$$

Note that when $P_{i,t}^{\mathrm{D}} < 0, \Delta C_{i,t}^k = 0$.

To summarize, at transaction time t, MG i in the NP (i.e., the bid inviter) announces a makeup price $\Delta C_{i,t}^k$. The MGs in the SP (i.e., qualified bidders) give their prices C_o^k. The bid inviter chooses the lowest price $C_{o1,t}^k$ and pays bidder $o1$ at price $\Delta C_{i,t}^k + C_{o1}^k$. If bidder o1 cannot cover the demand of the bid inviter, the rest of the demand will be covered by bidder $o2$ with the second lowest price C_{o2}^k and so on. Thus, the total payment of the bid inviter is $(\Delta C_{i,t}^k + C_{o1}^k)P_{o1} + (\Delta C_{i,t}^k + C_{o2}^k)P_{o2} + \ldots$, where P_o is the amount of the supply offered by bidder o. This bidder o chooses the highest makeup price $\Delta C_{i1,t}^k$ and charges bid inviter $i1$ at price $\Delta C_{i1,t}^k + C_o^k$. If bid inviter $i1$ cannot cover the supply of bidder o, the rest of bidder o's supply will be covered by bid inviter $i2$ with the second highest makeup $\Delta C_{i2,t}^k$, and so on. Then the total income of bidder o is

$(\Delta C^k_{i1,t} + C^k_o)P_{i1} + (\Delta C^k_{i2,t} + C^k_o)P_{i2} + ...$, where P_i is the amount of the demand requested by bid inviter i.

5.2. Game vector

We define the exchange variable $p^{e,f}_{i,n,t}$, which denotes the exchanged energy or rented storage capacity e from MG i to MG n at node f. Here, e stands for one of the six energy types that take part in the game vector: $P^{\text{SBRE}}_{f,t}$ ($e = 1$), $P^{\text{SBIN}}_{f,t}$ ($e = 2$), $P^{\text{SBLE}}_{f,t}$ ($e = 3$), $P^{\text{SBOUT}}_{f,t}$ ($e = 4$), $P^{\text{rin}}_{f,t}$ ($e = 5$), and $P^{\text{rout}}_{f,t}$ ($e = 6$). Moreover, C^k_i is defined as the base trade price of the tradable energy or service class k from MG i, where k stands for one of three classes: renewable generation ($k = 1$), the energy stored in each MG's own ESS ($k = 2$), and rented stored energy or storage capacity ($k = 3$). The game vector of MG i is $[P^{\text{BSRE}}_{i,t}\ P^{\text{w.sin}}_{i,t}\ P^{\text{BSIN}}_{i,t}\ P^{\text{BSLE}}_{i,t}\ P^{\text{w.sout}}_{i,t}\ P^{\text{BSOUT}}_{i,t}]$, which includes all of its tradable energy and service as decision variables. The game vector is based on a two-stage decision making process, where the priority-based determination in each stage is realized with the help of the binary condition variables (i.e., $a^r_{i,t}$ and $x^r_{o,i,t}$). In the first stage, $a^r_{i,t}$ is utilized to decide whether the first three decision variables in the game vector are in the NP. If more than one decision variable is in the NP, then which one will be calculated first must be determined. Similarly, 1- $a^r_{i,t}$ is utilized to decide whether the last three decision variables are in the SP. Take $P^{\text{w.sin}}_{i,t}$ for example. If $a^2_{i,t} = 1$,$P^{\text{w.sin}}_{i,t}$ is kept in the second stage for calculation, which means that a decision to purchase renewable energy has been made. In the second stage, a reserved decision variable in the NP (SP) has a decision set, where each element represents the tradable energy and service of another MG available to trade with MG i. In addition, $x^r_{o,i,t}$ is utilized to determine the priority of the transactions with the available MGs according to the proposed bidding mechanism. Mathematically, the above decision making process is expressed in (20)–(26) with the 4 sub-conditions of $x^r_{o,i,t}$.

In (7), the decision variables $P^{\text{SBRE}}_{f,t}$,$P^{\text{SBIN}}_{f,t}$,$P^{\text{SBLE}}_{f,t}$,$P^{\text{SBOUT}}_{f,t}$,$P^{\text{rin}}_{f,t}$, and $P^{\text{rout}}_{f,t}$ result from the multiplication of two game vectors: the binary condition variable-based game vector and the decision variable-based game vector. To analyze the trade decision and build the game vector, $P^{\text{rin}}_{f,t}$ is taken as an example. The expression for $P^{\text{rin}}_{f,t}$ is written as

$$P^{\text{rin}}_{f,t} = X^2_{f,t}P^2_{f,t} \tag{20}$$

$$X^2_{f,t} = [...x^{2,f}_{o,i,t}...x^{2,f}_{O,i,t}] \tag{21}$$

$$P^2_{f,t} = [...p^{2,f}_{o,i,t}...p^{2,f}_{O,i,t}]^{\text{T}} \tag{22}$$

$$x^{2,f}_{o,i,t} = \begin{cases} 1 & \text{condition } x'^{2,f}_{o,i,t} \\ 0 & \text{others} \end{cases} \tag{23}$$

where $X^2_{f,t}$ represents the game vector of binary decision variables corresponding to $P^2_{f,t}$. Priority condition $x'^{2,f}_{o,i,t}$ can be described as follows.

During trade decision making, the first step is to determine the game set [37].The binary variable $1-a^2_{i,t}$ classifies the decision variable $p^{o,i,t}_2$ into two game sets: the SP and non-SP sets. Similarly, $a^2_{i,t}$ classifies the decision variable $p^{2,f}_{o,i,t}$ into two game sets: the NP and non-NP sets. if the need-supply pool pairs—i.e., the game set—are determined at time t for $P^2_{f,t}$, the next step is to build the game vector based on the proposed trade mechanism. The initialization of a game vector is defaulted as zeros in the vector. After the game vector is built, each element value in the vector is determined. In the determined NP, price signal $\Delta C^2_{i,t}$ of MG i is utilized to determine its purchase priority, while in the determined SP, price signal C^2_o of MG o is used to determine its sale priority. This means the MG with a lower $C^2_o + \Delta C^2_{i,t}$ can sell its energy or service with a higher priority.

The condition $x'^{2,f}_{o,i,t} = 1$ can be described as the following sub-conditions.

Sub-condition 1: $(1-a^2_{o,t}) = 1$,$a^2_{i,t} = 1$,$\Delta C^2_{i,t} = \max\{\Delta C^2_{i',t}\ |i' \in \text{NP}\}$, and $C^2_o = \min\{C^2_{o'}\ |o' \in \text{SP}\}$.

Sub-condition 2: when $\Delta C^2_{i,t} = \max\{\Delta C^2_{i',t}\ |i' \in \text{NP}\}$and $C^2_o \neq \min\{C^2_{o'}\ |o' \in \text{SP}\}$,$\sum_{f\in M_i}(P^{\text{L}}_{f,t} - P^{\text{r,s}}_{f,t}) > \sum_{o'\in O'}\sum_{f\in M_{o'}} p^{2,f}_{o',i,t}$,$\forall\ o'. \in \{o' | C^2_{o'} < C^2_o\}$

Sub-condition 3: when $\Delta C^2_{i,t} \neq \max\{\Delta C^2_{i',t}\ |i' \in \text{NP}\}$and $C^2_o = \min\{C^2_{o'}\ |o' \in \text{SP}\}$,$\sum_{i'\in I'}\sum_{f\in M_{i'}}(P^{\text{L}}_{f,t} - P^{\text{r,s}}_{f,t}) < \sum_{f\in M_o} p^{2,f}_{o,i,t}$,$\forall\ i'. \in \{i' | C^2_{i'} < C^2_i\}$

Sub-condition 4: when $\Delta C^2_{i,t} \neq \max\{\Delta C^2_{i',t}\ |i' \in \text{NP}\}$and $C^2_o \neq \min\{C^2_{o'}\ |o' \in \text{SP}\}$,$\sum_{i'\in I'}\sum_{f\in M_{i'}}(P^{\text{L}}_{f,t} - P^{\text{r,s}}_{f,t}) > \sum_{o'\in O'}\sum_{f\in M_{o'}} p^{2,f}_{o',i,t}$.

By analogy with $x'^{2,f}_{o,i,t}$, we can obtain all conditions of the proposed game vector, i.e., $x'^{e,f}_{i,o,t}$ (when $e = 1, 2, 3$), and $x'^{e,f}_{o,i,t}$ (when $e = 4, 5, 6$). So all decision variables $P^{\text{SBRE}}_{f,t}$,$P^{\text{SBIN}}_{f,t}$,$P^{\text{SBLE}}_{f,t}$,$P^{\text{SBOUT}}_{f,t}$,$P^{\text{rin}}_{f,t}$, and $P^{\text{rout}}_{f,t}$ are presented in the following

$$X^e_{f,t}P^e_{f,t} = \begin{cases} [...x^{e,f}_{o,i,t}...x^{e,f}_{O,i,t}][...p^{e,f}_{o,i,t}...p^{e,f}_{O,i,t}]^{\text{T}} & e = 1,2,3 \\ [...x^{e,f}_{i,o,t}...x^{e,f}_{i,O,t}][...p^{e,f}_{i,o,t}...p^{e,f}_{i,O,t}]^{\text{T}} & e = 4,5,6 \end{cases} \tag{24}$$

$$x^{e,f}_{o,i,t} = \begin{cases} 1 & \text{condition } x'^{e,f}_{o,i,t} \\ 0 & \text{others} \end{cases} \quad e = 1,2,3 \tag{25}$$

$$x^{e,f}_{i,o,t} = \begin{cases} 1 & \text{condition } x'^{e,f}_{i,o,t} \\ 0 & \text{others} \end{cases} \quad e = 4,5,6 \tag{26}$$

6. Algorithm solution

The proposed pricing model is a bilevel programming model with mixed integers. Most analytical methods cannot solve this type of model in a reasonable computation time and obtain an optimum solution. However, genetic algorithm (GA)-based methods have been successfully and widely applied to complex practical optimization problems with enhanced convergence performance [38,37]. In this paper, the

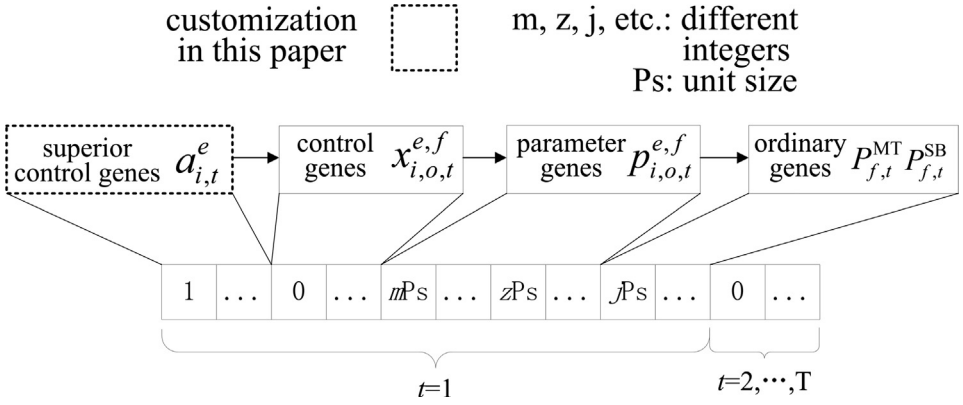

Fig. 4. Chromosome coding of the customized hierarchical genetic algorithm.

authors have customized the NSGA-II-based traditional hierarchical genetic algorithm (HGA) to make it more suitable for the type of variables and relationships in the current work to solve the proposed mixed-integer programming problem. In an HGA, the chromosome coding has two layers: the control gene layer and the parameter gene layer. Control genes are encoded by binaries to control parameter genes. Parameter genes are encoded by real numbers to represent decision variables. When a control gene is set to 1, the corresponding parameter gene is activated. Ordinary genes are also in chromosome coding encoded by real numbers and they are independent of those two types of genes. To better solve the problem, a customized HGA (C-HGA) is presented that adds a superior control gene layer upon the existing control gene layer to manage the control genes. When a superior control gene is set to 1, the corresponding control gene is activated.

6.1. Customization: chromosome representation

For the proposed model, the C-HGA chromosome coding is expressed in Fig. 4. The superior control genes are the binary condition variables in (15)–(17) that determine the SP and the NP. The control gene is $x_{o,i,t}^{e,f}$. The decision variable $p_{o,i,t}^{e,f}$ is the parameter gene. $P_{f,t}^{\mathrm{MT}}$ and $P_{f,t}^{\mathrm{SB}}$ are the ordinary genes.

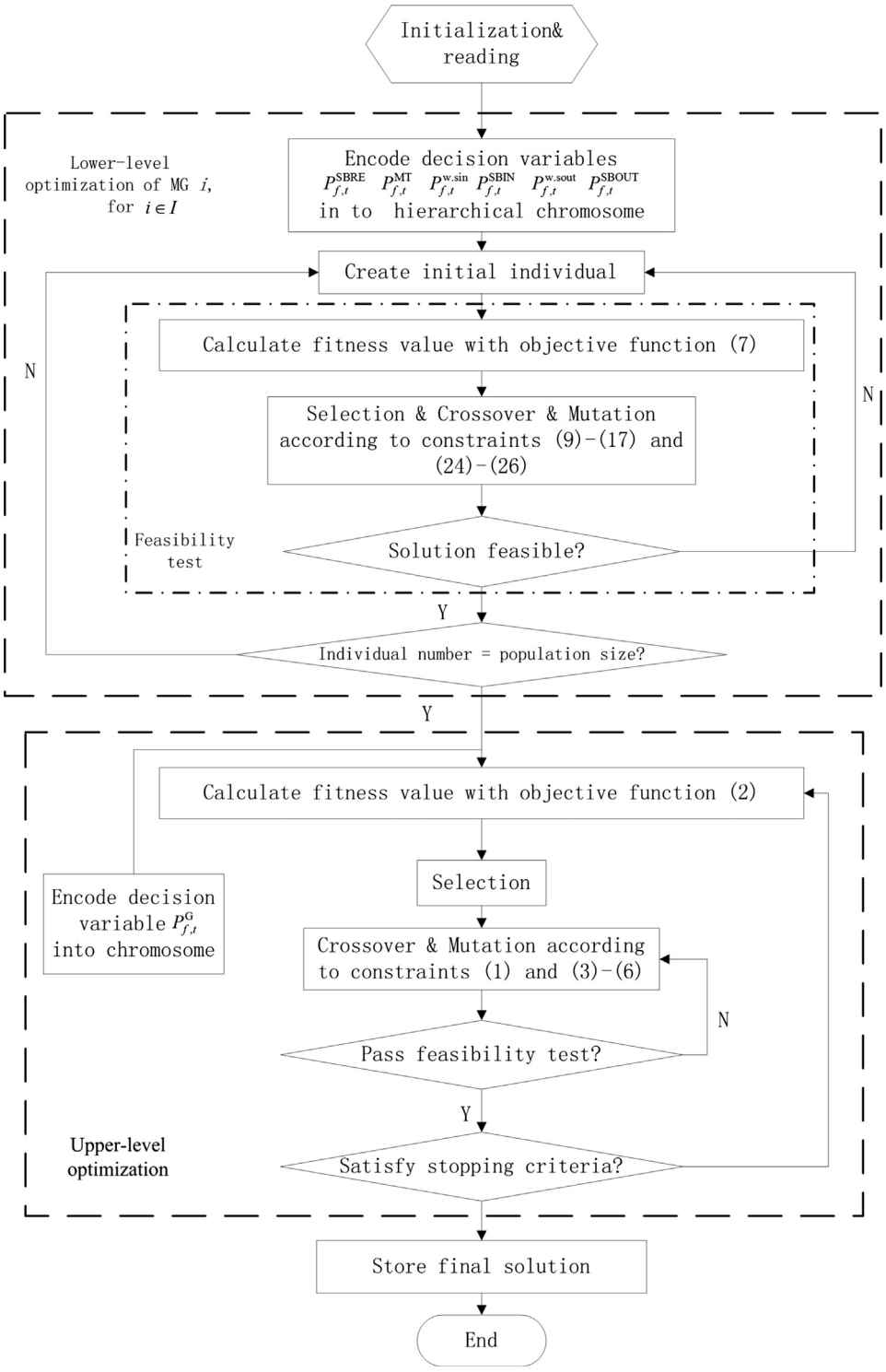

Fig. 5. Flow chart of the proposed algorithm.

The customized chromosome representation is made for the proposed game vector. The establishment of a group of genes in a customized chromosome is based on priority. First, the value of gene $a_{i,t}^{e}$ is determined according to conditions (15)–(17). Second, the value of gene $x_{o,i,t}^{e,f}$ is determined by conditions (25) and (26). Finally, the decision variable $p_{o,i,t}^{e,f}$ is calculated considering $a_{i,t}^{e}$ and $x_{o,i,t}^{e,f}$.

6.2. Solution procedure

Solution feasibility check: (1) Substitute every exchange variable (i.e., $P_{f,t}^{\mathrm{TL}}$) of an individual in the upper level into the lower level and calculate the lower model with the C-HGA. (2) Check whether there is a solution of the optimization problem in the lower level.

Step 0: Initialization. Set the chromosome, population size, and generation = 1.
Step 1: Create initial population. Inspect individuals with solution feasibility check. Update individuals that do not pass the check with the same number of new individuals until all individuals in the population pass the check.
Step 2: Calculate fitness values according to objective function (2).
Step 3: Let the current generation of the population do selection during upper-level optimization.
Step 4: Let the current generation of the population do crossover and mutation during upper-level optimization. Check the solution feasibility of the generated individuals. Eliminate individuals that lead to infeasible solutions, and continue crossover and mutation until the next generation of the population is formed.
Step 5: If the convergence condition is satisfied, return the optimal solution and the algorithm ends; otherwise go to step 2.

The flow chat of the proposed algorithm is depicted in Fig. 5.

Table 1
Device parameters of the MGs.

WT rated output (kW)	PV rated output (kW)	SB max output (kW)	SB capacity (kWh)	MT max output (kW)
260	185	90	280	185

Table 2
Energy and service price of the MGs.

MG	C_i^1 ($/kWh)	C_i^2 ($/kWh)	C_i^3 ($/((kWh) h))
$i = 1$	0.125	0.17	0.015
$i = 2$	0.12	0.175	0.0125
$i = 3$	0.11	0.18	0.01

7. Case studies

In this section, a modified IEEE 33-bus feeder is taken as the main test system. A second real-world test system is also presented to provide additional evidence of the suitability of the proposed model.

7.1. Description of main test system

As shown in Fig. 6, topology extensions for three MGs are connected to the original IEEE 33-bus feeder. Details concerning the IEEE 33-bus test system can be found in [31]. For this test system, the voltage base was 10.5 kV, the total active load was 2963 kW, and the total reactive load was 785 kVAR. Three 250 kW MTs and two −150 to 350 kVAR SVCs were connected to the distribution network. Table 1 summarizes the device parameters of the MGs. Operating cost parameters of the DGs and the ESS can be obtained from [39]. A 2 m-point estimate method (2 m-PEM) [40] was used in this paper to build the approximate formulation for uncertainty in renewable generation. A normal

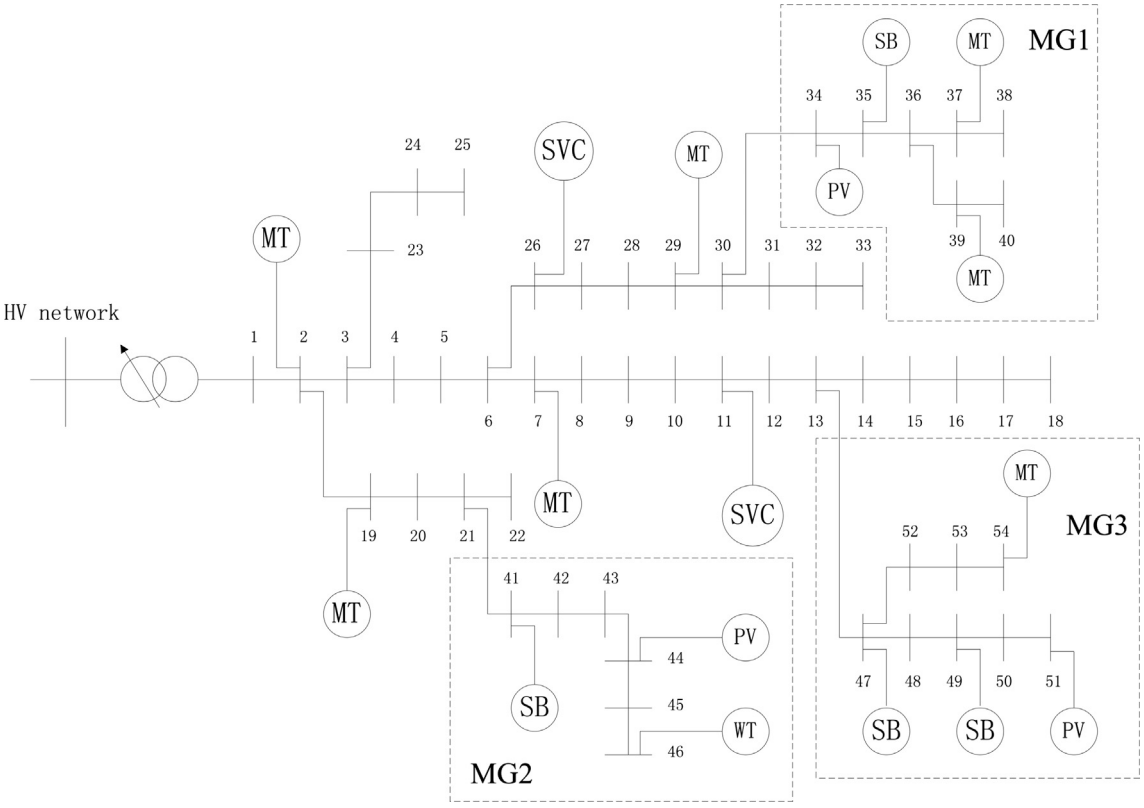

Fig. 6. Single line diagram of the modified IEEE 33-bus feeder with MG topology extensions.

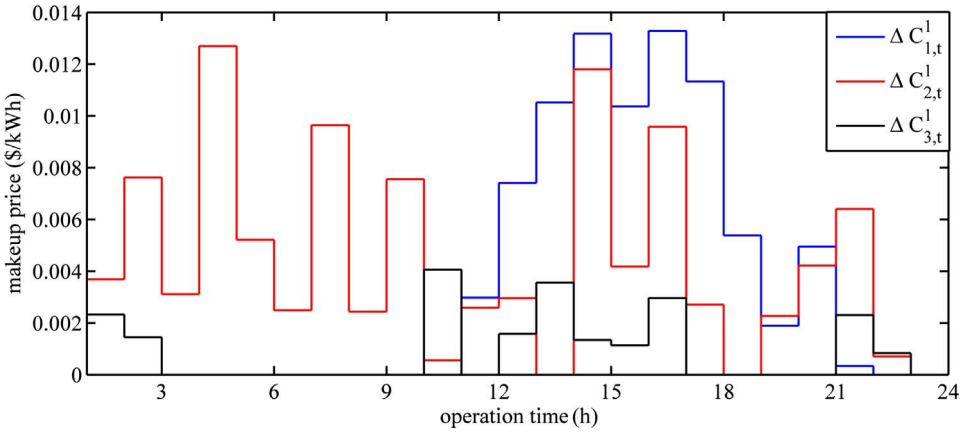

Fig. 7. The dynamic makeup price ($k = 1$) of MG1, MG2, and MG3.

Table 3
Case information.

MG(s) in the system	Strategy 1	Strategy 2	Strategy 3	Strategy 4	Strategy 5
MG1	Case 1	Case 3	–	–	–
MGs 1–3	Case 2	Case 4	Case 5	Case 6	Case 7

distribution is frequently used to represent the forecasting uncertainty of load consumptions, in which the mean value of the normal distribution is the forecasted load and the standard deviation is set to be 2% of the expected load [41]. The bidding prices are outlined in Table 2. Fig. 7 shows an example of one dynamic makeup price ($k = 1$) of MG1, MG2, and MG3. Other makeup prices can be calculated according to (19).

To demonstrate the proposed strategy, the following pricing strategies and cases were considered in this paper:

Strategy 1: the proposed pricing strategy
Strategy 2: the traditional centralized dispatch strategy, whose objective is to minimize the total operational costs of the distribution network and MGs with constraints (1) and (3)–(6)
Strategy 3: the proposed pricing mechanism without the first and fourth item of the objective function (2) and the constraint (1), which means that this strategy does not consider the operational quality
Strategy 4: the traditional game model proposed in [42]
Strategy 5: the deterministic model of the proposed strategy, which ignores the renewable uncertainty
Case 1: strategy 1 is applied to the distribution system including one MG (MG1)
Case 2: strategy 1 is applied to the distribution system including three MGs (MG1, MG2, and MG3)
Case 3: strategy 2 is applied to the system in case 1
Case 4: strategy 2 is applied to the system in case 2
Case 5: strategy 3 is applied to the system in case 2
Case 6: strategy 4 is applied to the system in case 2
Case 7: strategy 5 is applied to the system in case 2

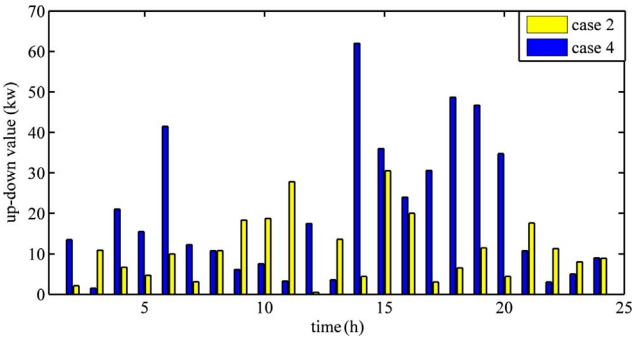

Fig. 9. Comparison of power fluctuation smoothing in cases 2 and 4.

Table 3 illustrates the cases under different strategies and systems, where strategy 1 (case 1) is benchmarked against strategies 2–5 (cases 4–7) to analyze multiple performances of the proposed pricing mechanism. For power exchange analysis, cases 1 and 2 are benchmarked against cases 3 and 4.

All calculations were performed on a PC with a 3.4-GHz Intel Core i7 processor and 16 GB of RAM using the GAMS environment integrated with MATLAB, which codes the C-HGA.24 trading transactions are assumed every day with the time interval of 1 h. One day of 24 intervals is considered in the simulations.

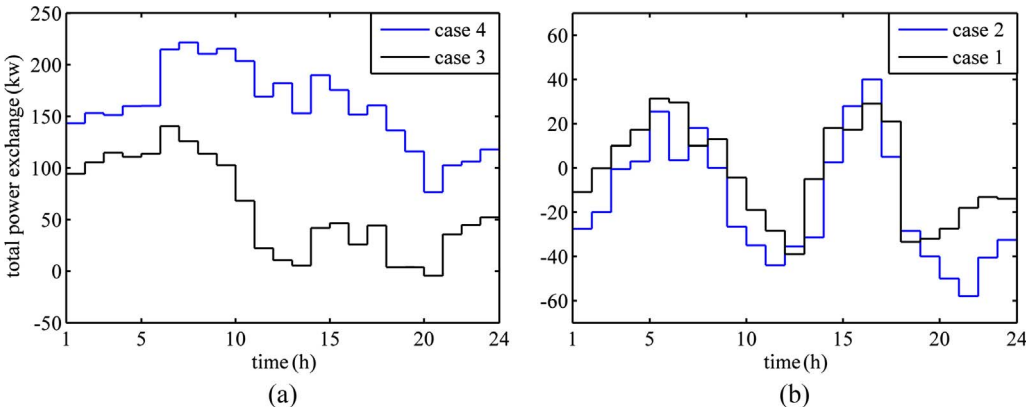

Fig. 8. Total power exchange for different cases: (a) case 3 (s% = 6.7%) and case 4 (s % = 18.4%) and (b) case 1 (s% = 6.7%) and case 2 (s% = 18.4%).

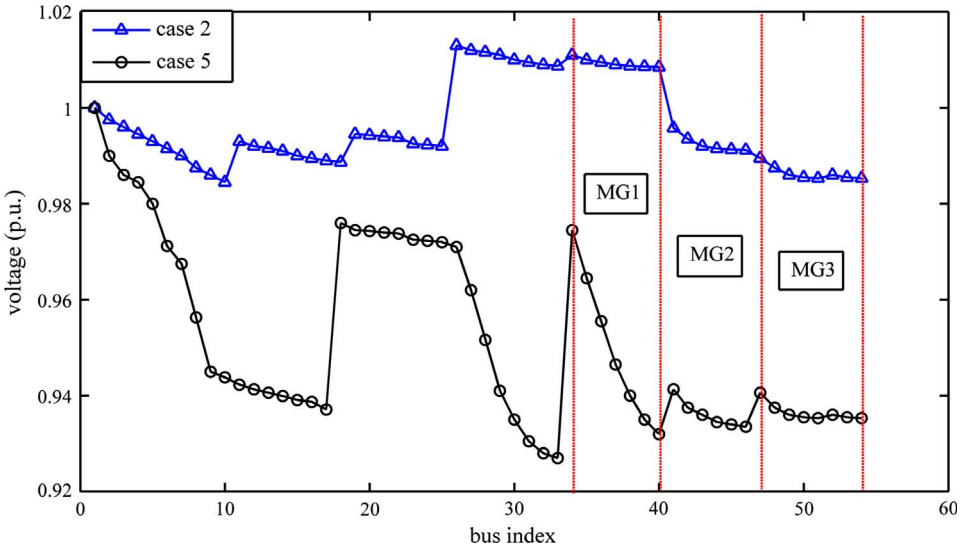

Fig. 10. Voltage profiles in two cases.

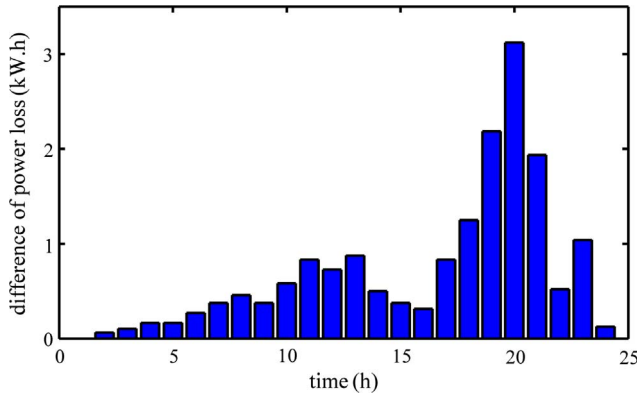

Fig. 11. Comparison of power losses in case 2 and case 4.

Table 4
Economic performance of each entity under different strategies.

	Case 4 ($)	Case 6 ($)	Case 2 ($)
MG1	−485.3	−489.7	−480.2
MG2	−631.3	−603.6	−575.1
MG3	−366.5	−341.9	−334
DEMO	509.9	403.6	518.4
Total	−973.2	−1031.6	−870.9
ST (s)	103.8	473	509

Table 5
Economic performance of case 7 and case 2.

Pricing strategy	Case 7	Case 2
Cost of MGs ($)	1106.7	1389.3
DEMO profit ($)	501.8	518.4
Total cost ($)	604.9	870.9
ST (s)	466	609

7.2. Sensitivity analysis between penetration level and power exchange

The penetration level of renewable generation and the fluctuation in power of the total power exchange between MGs and the distribution network are important indices to evaluate the reliability and expandability of a distribution system. The fluctuation of the power exchange can be used to assess the accommodation capability of a distribution system to different penetration levels of renewables. If the fluctuation is very high under high-level penetrations, the power quality of the distribution network will be negatively affected. Here, we define s% as the penetration level of renewable generation, and 0.01s is the proportion of renewable generator capacity to annual load peak. If the number of MGs with renewable generators increases, s becomes higher.

Fig. 8(a) depicts the total power exchange in cases 3 and 4. As the grid price is less than the operational cost of an ESS, the fluctuation in renewable generation and loads is offset by the power exchange with the distribution network. When *s* is higher, the total power exchange increases significantly between −10 kW and 230 kW. However, as illustrated in Fig. 8(c), the fluctuation in renewable generation and loads is offset by the market interaction among MGs. So the growth of *s* has a smaller impact on the distribution network. The total power exchange is thus within a smaller range between −60 kW and 40 kW.

In addition, to quantify this smoothing effect on power fluctuations, the up–down fluctuation value of the total power exchange is defined as

$$P_t^{\text{up-down}} = |\sum_{f\in I} P_{f,t+1}^{\text{TL}} - \sum_{f\in I} P_{f,t}^{\text{TL}}| \tag{27}$$

As shown in Fig. 9, the power fluctuation is better smoothed in the proposed method compared to the traditional dispatch strategy.

7.3. Voltage profile

Fig. 10 shows 24 h mean voltage values at all buses. We can see that system voltage deviations are reduced due to the reactive compensation of the SVCs at bus 11 and bus 26 and the reactive generation of the DGs. The voltage deviations range from 0.98 p.u. to 1.02 p.u. On the other hand, strategy 3 leads to voltage violations (−0.5 p.u. +0.5 p.u.) without operation optimizations.

7.4. Power loss

Fig. 11 shows the power loss in case 2 versus power loss in case 4. We can see that all the differences are positive and that during peak hours (18 h–21 h), the differences are especially high. This means that, compared to case 4, the power loss of the distribution system in case 2 is effectively reduced with the adjustment of energy trade.

7.5. Economic performance

In Table 4, we compare three cases in terms of each entity's profit (+)/cost(−) and the simulation time (ST). The centralized formulation

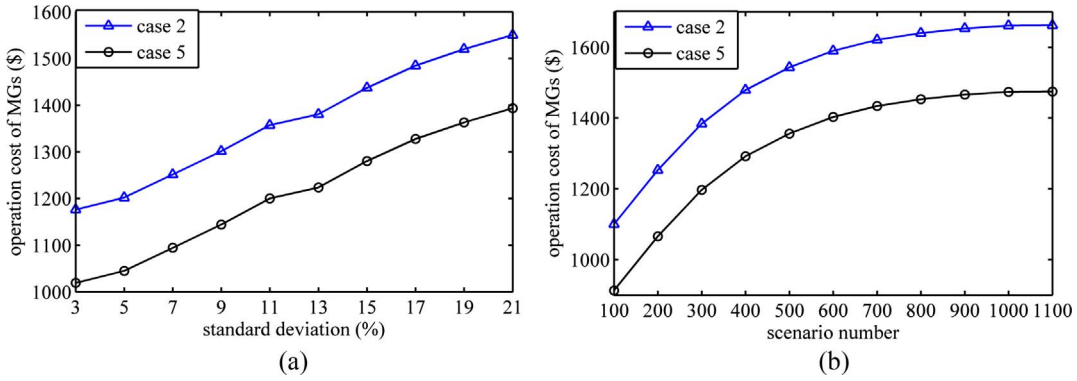

Fig. 12. Sensitivity analysis: (a) total operational cost of the MGs versus standard deviation of renewable generation forecasting error and (b) total operational cost of the MGs versus number of scenarios.

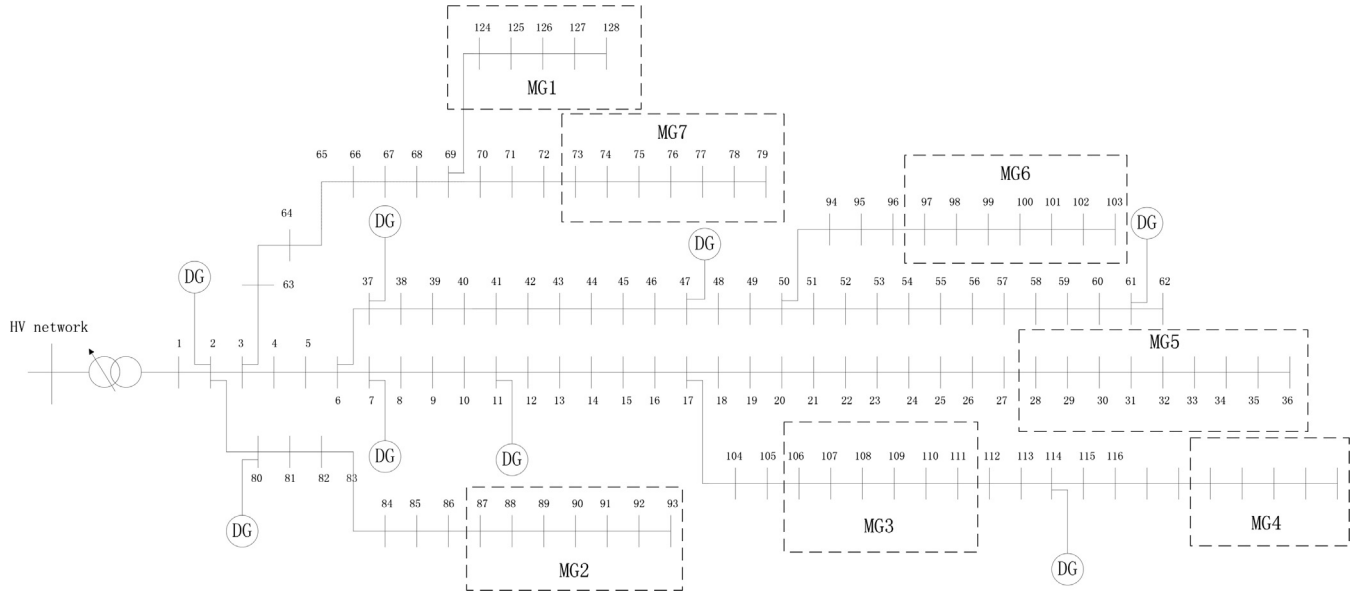

Fig. 13. Single line diagram of a real system.

Table 6
Configuration of MGs.

MG	WT nominal rating (kW)	PV nominal rating (kW)	WT&PV normalized standard deviation (%)	SB total maximum output (kW)	SB total capacity (kWh)	MT total maximum output (kW)	FC total maximum output (kW)
MG1-2	800	750	5.1	500	1500	300	500
MG3-4	750	500	5.3	500	1500	200	850
MG5-7	1000	1200	5.0	1000	2500	800	1000

(case 4) has a higher summation of all profits (lower costs) than the traditional game model (case 6). This is because the objective of strategy 2 is to minimize the operational costs of all entities, while the benefits of some entities may be sacrificed to achieve equilibrium in the traditional game theory formulation.

In the proposed formulation, the total cost of case 2 is higher than in case 6 and in case 4. This is because the dynamic makeup $\Delta C_{i,t}^{k}$ and trade price C_i^k is introduced to facilitate market interactions among MGs. More energy and storage services are traded under the proposed game vector-based trade mechanism at a higher price, thus resulting in more profits.

Due to more information and higher dimensions in each computation iteration, the proposed pricing strategy takes more ST than the other two benchmarks. Since more profits and better operational quality are obtained under this strategy, the ST is acceptable for medium to short term market regulation with hour-level response.

7.6. Stochasticity analyses

To analyze the stochasticity impact on economic operations, strategy 1 and strategy 5 are compared. In Table 5, we can see that the total operational costs of the stochastic model (case 2) are higher than with the deterministic model (case 7). The main economic differences between case 2 and case 7 exist in the cost of the MGs, since the MGs include intermittent renewable resources. This is expected since the optimal value of a deterministic optimization is biased upward relative to one of the corresponding stochastic optimizations according to Jensens inequality [43]. The difference between the optimal values of the deterministic and stochastic models is the value of the perfect information.

Sensitivity analyses of the operational costs of the MGs under different standard deviations of the renewable generation prediction and different scenario numbers are conducted in Fig. 12 to further explore

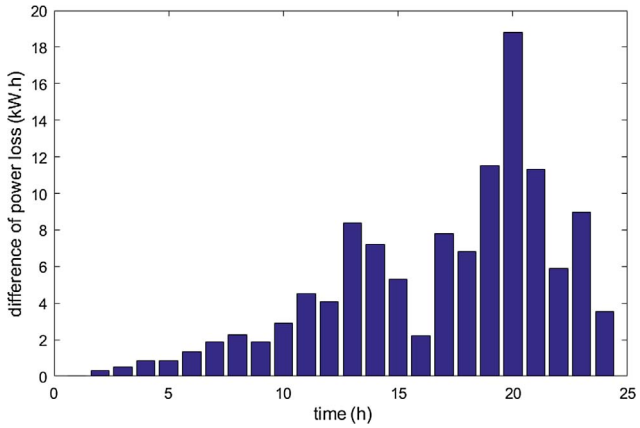

Fig. 14. Comparison of power losses in strategy 1 and strategy 2.

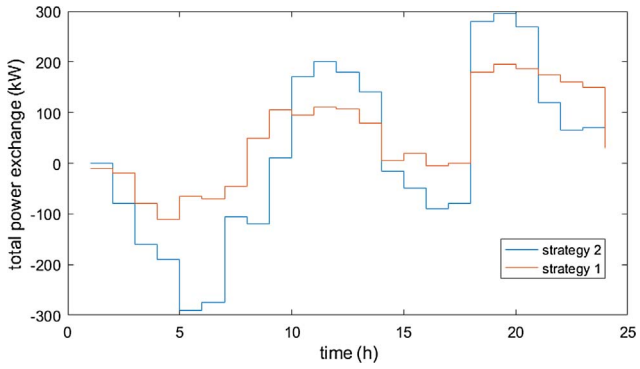

Fig. 15. Total power exchange curves in strategy 1 and strategy 2.

the stochastic impact on market operation.

Fig. 12(a) shows that a higher variance in renewable generation leads to higher operational costs of the MGs. This is expected because a higher variance implies that there is a higher probability to have a lower realization of renewable generation given a constant number of scenario samplings. Fig. 12(b) demonstrates that the operational cost of the MGs converges as the number of scenarios increases. This is because an infinite scenario number for case 2 results in an unbiased and consistent estimator of (18) [43], which means the operational dispatch under the proposed pricing strategy is more robust.

7.7. Test on real-world system

The proposed pricing mechanism was applied to a real distribution energy system with 7 energy hubs (MGs) in Shandong Province, China. The single line diagram of the real system is shown in Fig. 13.

The data concerning the equipment participating in the test are shown in Table 6.

The remaining data and parameters are found in the previous case study. Fig. 14 shows the power loss in strategy 1 versus power loss in strategy 2. Similar to Fig. 11, all the differences are positive and that during peak hours (13 h-15 h and 19 h21 h), the differences are especially high.

Similar to Fig. 8, Fig. 15 shows that the total power exchange between MGs and the distribution network in strategy 1 is smoothed compared with that in strategy 2.

Table 7 shows that the standard deviation of the 24 h power fluctuation is reduced by 62.2% compared with strategy 2 when the proposed pricing strategy is adopted. Furthermore, the average voltage profile is improved to 31.1% of the voltage profile in strategy 2, and the average power loss is reduced to 11.7% of the power loss. Although the simulation time in strategy 1 is 28.8% more than that of strategy 2, it is still acceptable considering the advantage the proposed strategy brings in its application of short- to medium-term market regulation.

7.8. Real application

In addition to the above test, the real application of the proposed pricing mechanism was implemented on a day-ahead market through a market operator system of the above real system in practical operations. As shown in Figs. 16(a) and (b), the market operator has two layers: a transaction supervision (TS) layer and a control layer. Firstly, the proposed pricing mechanism in the TS layer produces a day-ahead transaction plan. Then the entire transaction plan is divided into multi-short intervals. According to the first interval of the plan and real-time generation/load/trading data, the control layer gives a signal of revisionary reference values to controllers of the ESSs and controllable DGs to control them in real time. When this control process is completed in that interval, the control layer gives another signal in the next interval according to the next interval plan and real-time data until the last control process is completed in the last interval. The above coordinated transaction-based dispatch is a kind of receding horizon optimization [44]. Hence, the real-time output of the ESSs and controllable DGs can follow the transaction plan through the control layer. Figs. 16(c)–(e) show major equipment facilities.

8. Conclusion

In this paper, a dynamic pricing mechanism that achieves multi-optimal operational performance in coupled MG-based smart energy systems was proposed that also considers the uncertainty of large-scale renewable integration. A two-level optimization was developed, which describes market operations of the DEMO in the upper level and the MGs in the lower level. The upper-level model improves the operation quality of distribution systems, such as power exchange (Section 7.2), voltage profile (Section 7.3), power loss (Section 7.4), and profitable trade benefits (Section 7.5) through interactions with the MGs. The lower-level model maximizes the profit of each MG and represents the prediction error inherent with renewable generation. A game vector was proposed to mimic the trade decisions and model the market interactions of each MG. An interactive transaction mechanism was established to promote market interactions based on tradable energy and storage services, and a dynamic makeup price. A customized HGA was used to solve the proposed hierarchical model. Simulations conducted using a modified IEEE 33-bus system and further simulations using a real-world energy system in China demonstrated the effectiveness of the proposed methodology. Under a high penetration of renewable integration, the proposed pricing mechanism optimized each entity's profit and system-level operational performance.

Table 7
Simulation results.

Strategy	Standard deviation of 24 h power fluctuation (kW)	All-bus-average standard deviation of 24 h voltage (p.u.)	24 h-average power loss of the system (kWh)	Total operation cost ($)	ST (s)
1	43.64	0.031	62.93	36987.28	904
2	110.39	0.045	71.21	37469.12	702

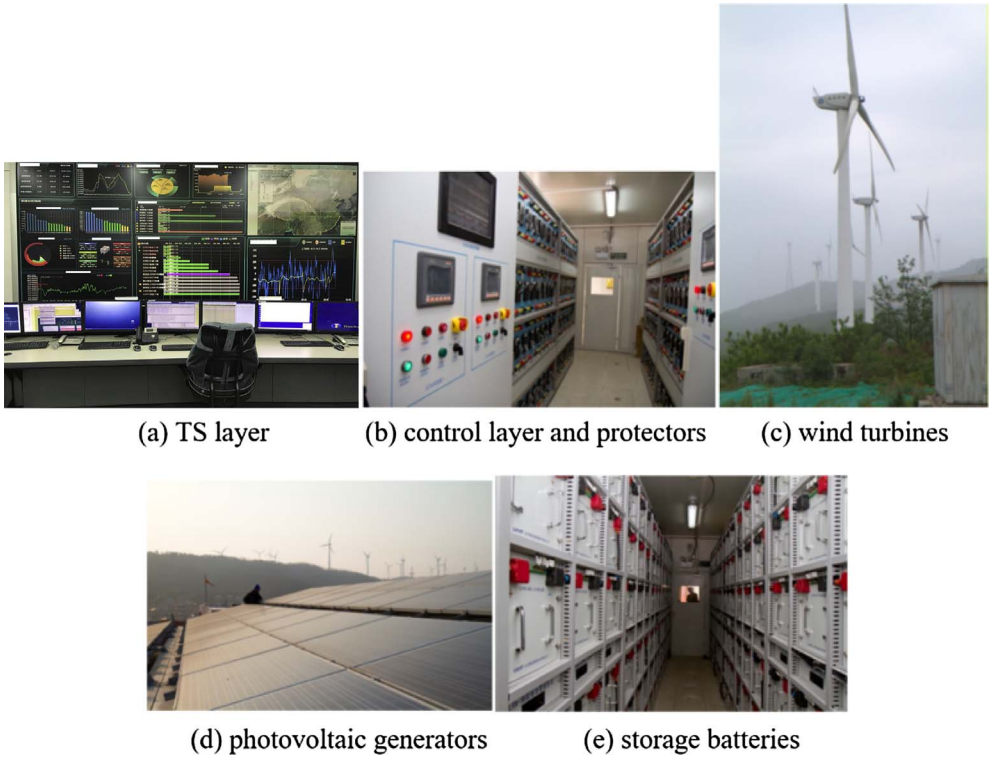

Fig. 16. Figures of the real system.

Acknowledgements

This work was partially supported by the National Natural Science Foundation of China under Grant 51577115 and U1766207. Z. Wang's work is supported by the U.S. Department of Energy Office of Electricity Delivery and Energy Reliability under DE-OE-0000839.

References

[1] Lee Y, Kim C, Shin J. A hybrid electric vehicle market penetration model to identify the best policy mix: a consumer ownership cycle approach. Appl Energy 2016;184(Supplement C):438–49. http://dx.doi.org/10.1016/j.apenergy.2016.10.038 http://www.sciencedirect.com/science/article/pii/S0306261916314787 .

[2] Armendriz M, Heleno M, Cardoso G, Mashayekh S, Stadler M, Nordstrm L. Coordinated microgrid investment and planning process considering the system operator. Appl Energy 2017;200:132–40. http://dx.doi.org/10.1016/j.apenergy.2017.05.076 http://www.sciencedirect.com/science/article/pii/S030626191730569X .

[3] Ding T, Lin Y, Bie Z, Chen C. A resilient microgrid formation strategy for load restoration considering master-slave distributed generators and topology reconfiguration. Appl Energy 2017;199:205–16. http://dx.doi.org/10.1016/j.apenergy.2017.05.012 http://www.sciencedirect.com/science/article/pii/S0306261917305056 .

[4] Bustos C, Watts D. Novel methodology for microgrids in isolated communities: Electricity cost-coverage trade-off with 3-stage technology mix, dispatch and configuration optimizations. Appl Energy 2017;195:204–21. http://dx.doi.org/10.1016/j.apenergy.2017.02.024 http://www.sciencedirect.com/science/article/pii/S0306261917301447 .

[5] Akhtar Z, Saqib MA. Microgrids formed by renewable energy integration into power grids pose electrical protection challenges. Renew Energy 2016;99(Supplement C):148–57. http://dx.doi.org/10.1016/j.renene.2016.06.053 http://www.sciencedirect.com/science/article/pii/S0960148116305778 .

[6] Dalkilic O, Candogan O, Eryilmaz A. Dayahead electricity pricing for a heterogeneous microgrid under arbitrary utility and cost structures. IEEE Trans Smart Grid PP 2016(99):1. http://dx.doi.org/10.1109/TSG.2016.2552150.

[7] Papadaskalopoulos D, Strbac G. Nonlinear and randomized pricing for distributed management of flexible loads. IEEE Trans Smart Grid 2016;7(2):1137–46. http://dx.doi.org/10.1109/TSG.2015.2437795.

[8] Anees A, Chen Y-PP. True real time pricing and combined power scheduling of electric appliances in residential energy management system. Appl Energy 2016;165:592–600. http://dx.doi.org/10.1016/j.apenergy.2015.12.103 http://www.sciencedirect.com/science/article/pii/S0306261915016761 .

[9] Aghajani G, Shayanfar H, Shayeghi H. Presenting a multi-objective generation scheduling model for pricing demand response rate in micro-grid energy management. Energy Convers Manage 2015;106:308–21. http://dx.doi.org/10.1016/j.enconman.2015.08.059 http://www.sciencedirect.com/science/article/pii/S0196890415008134 .

[10] Liu N, Yu X, Wang C, Li C, Ma L, Lei J. An energy sharing model with price-based demand response for microgrids of peer-to-peer prosumers. IEEE Trans Power Syst PP 2017(99):1. http://dx.doi.org/10.1109/TPWRS.2017.2649558.

[11] Zhang C, Xu Y, Dong ZY, Wong KP. Robust coordination of distributed generation and price-based demand response in microgrids. IEEE Trans Smart Grid PP 2017(99):1. http://dx.doi.org/10.1109/TSG.2017.2653198.

[12] Gong C, Tang K, Zhu K, Hailu A. An optimal time-of-use pricing for urban gas: a study with a multi-agent evolutionary game-theoretic perspective. Appl Energy 2016;163(Supplement C):283–94. http://dx.doi.org/10.1016/j.apenergy.2015.10.125 http://www.sciencedirect.com/science/article/pii/S0306261915013653 .

[13] Anvari-Moghaddam A, Rahimi-Kian A, Mirian MS, Guerrero JM. A multi-agent based energy management solution for integrated buildings and microgrid system. Appl Energy 2017;203(Supplement C):41–56. http://dx.doi.org/10.1016/j.apenergy.2017.06.007 http://www.sciencedirect.com/science/article/pii/S0306261917307572 .

[14] Umeozor EC, Trifkovic M. Operational scheduling of microgrids via parametric programming. Appl Energy 2016;180(Supplement C):672–81. http://dx.doi.org/10.1016/j.apenergy.2016.08.009 http://www.sciencedirect.com/science/article/pii/S0306261916310960 .

[15] Shaaban M, Eajal A, El-Saadany E. Coordinated charging of plug-in hybrid electric vehicles in smart hybrid ac/dc distribution systems. Renew Energy 2015;82: 92–99. International conference on renewable energy: generation and applications (ICREGA 2014). http://dx.doi.org/10.1016/j.renene.2014.08.012. <http://www.sciencedirect.com/science/article/pii/S0960148114004716>.

[16] Afar S, Brotcorne L, Marcotte P, Savard G. Achieving an optimal trade-off between revenue and energy peak within a smart grid environment. Renew Energy 2016;91:293–301. http://dx.doi.org/10.1016/j.renene.2016.01.055 http://www.sciencedirect.com/science/article/pii/S0960148116300556 .

[17] Shi X, Variam HM. East asias gas-market failure and distinctive economicsa case study of low oil prices. Appl Energy 2017;195(Supplement C):800–9. http://dx.doi.org/10.1016/j.apenergy.2017.03.091 http://www.sciencedirect.com/science/article/pii/S0306261917303331 .

[18] Karlsson M, Gebremedhin A, Klugman S, Henning D, Moshfegh B. Regional energy system optimization potential for a regional heat market. Appl Energy 2009;86(4):441–51. http://dx.doi.org/10.1016/j.apenergy.2008.09.012 http://www.sciencedirect.com/science/article/pii/S0306261908002365 .

[19] Ito M, Takano A, Shinji T, Yagi T, Hayashi Y. Electricity adjustment for capacity market auction by a district heating and cooling system. Appl Energy 2017;206(Supplement C):623–33. http://dx.doi.org/10.1016/j.apenergy.2017.08.210 http://www.sciencedirect.com/science/article/pii/S0306261917312436 .

[20] Pellegrino S, Lanzini A, Leone P. Techno-economic and policy requirements for the market-entry of the fuel cell micro-chp system in the residential sector. Appl Energy 2015;143(Supplement C):370–82. http://dx.doi.org/10.1016/j.apenergy.2015.01.007 http://www.sciencedirect.com/science/article/pii/S0306261915000136 .

[21] Ding Z, Lee WJ. A stochastic microgrid operation scheme to balance between system reliability and greenhouse gas emission. IEEE Trans Ind Appl

2016;52(2):1157–66. http://dx.doi.org/10.1109/TIA.2015.2490619.
[22] Su W, Wang J, Roh J. Stochastic energy scheduling in microgrids with intermittent renewable energy resources. IEEE Trans Smart Grid 2014;5(4):1876–83. http://dx.doi.org/10.1109/TSG.2013.2280645.
[23] Nagarajan A, Ayyanar R. Design and scheduling of microgrids using benders decomposition. In: 2016 IEEE 43rd photovoltaic specialists conference (PVSC); 2016. p. 1843–7. http://dx.doi.org/10.1109/PVSC.2016.7749940.
[24] Jannati M, Hosseinian S, Vahidi B, Li G jie. A significant reduction in the costs of battery energy storage systems by use of smart parking lots in the power fluctuation smoothing process of the wind farms. Renew Energy 2016;87(Part 1):1–14. http://dx.doi.org/10.1016/j.renene.2015.09.054 http://www.sciencedirect.com/science/article/pii/S0960148115303335 .
[25] Min C, Kim M, Park J, Yoon Y. Game-theory-based generation maintenance scheduling in electricity markets. Energy 2013;55:310–8. http://dx.doi.org/10.1016/j.energy.2013.03.060 http://www.sciencedirect.com/science/article/pii/S0360544213002569 .
[26] Wang J, Zhou Z, Botterud A. An evolutionary game approach to analyzing bidding strategies in electricity markets with elastic demand. Energy 2011;36(5):3459–67. http://dx.doi.org/10.1016/j.energy.2011.03.050 http://www.sciencedirect.com/science/article/pii/S0360544211002180 .
[27] Tang J, Lam H, Aziz MA, Morad N. Palm biomass strategic resource managment a competitive game analysis. Energy 2017;118:456–63. http://dx.doi.org/10.1016/j.energy.2016.07.163 http://www.sciencedirect.com/science/article/pii/S0360544216310969 .
[28] Srinivasan D, Rajgarhia S, Radhakrishnan BM, Sharma A, Khincha H. Game-theory based dynamic pricing strategies for demand side management in smart grids. Energy 2017;126:132–43. http://dx.doi.org/10.1016/j.energy.2016.11.142 http://www.sciencedirect.com/science/article/pii/S0360544216317996 .
[29] Nwulu NI, Xia X. Implementing a model predictive control strategy on the dynamic economic emission dispatch problem with game theory based demand response programs. Energy 2015;91:404–19. http://dx.doi.org/10.1016/j.energy.2015.08.042 http://www.sciencedirect.com/science/article/pii/S0360544215011160 .
[30] Chen Y, Wei W, Liu F, Mei S. A multi-lateral trading model for coupled gas-heat-power energy networks. Appl Energy 2017;200:180–91. http://dx.doi.org/10.1016/j.apenergy.2017.05.060 http://www.sciencedirect.com/science/article/pii/S0306261917305147 .
[31] Baran ME, Wu FF. Network reconfiguration in distribution systems for loss reduction and load balancing. IEEE Trans Power Deliv 1989;4(2):1401–7. http://dx.doi.org/10.1109/61.25627.
[32] Wang Z, Chen H, Wang J, Begovic M. Inverter-less hybrid voltage/var control for distribution circuits with photovoltaic generators. IEEE Trans Smart Grid 2014;5(6):2718–28. http://dx.doi.org/10.1109/TSG.2014.2324569.
[33] Fathi M, Bevrani H. Statistical cooperative power dispatching in interconnected microgrids. IEEE Trans Sustain Energy 2013;4(3):586–93. http://dx.doi.org/10.1109/TSTE.2012.2232945.
[34] Tan S, Xu JX, Panda SK. Optimization of distribution network incorporating distributed generators: an integrated approach. IEEE Trans Power Syst 2013;28(3):2421–32. http://dx.doi.org/10.1109/TPWRS.2013.2253564.
[35] Kariuki KK, Allan RN. Evaluation of reliability worth and value of lost load. IEE Proc – Gener Transmiss Distrib 1996;143(2):171–80. http://dx.doi.org/10.1049/ip-gtd:19960191.
[36] Valente C, Mitra G, Sadki M, Fourer R. Extending algebraic modelling languages for stochastic programming. INFORMS J Comput 2009;21(1):107–22.
[37] Joe-Wong C, Kamitsos I, Ha S. Interdatacenter job routing and scheduling with variable costs and deadlines. IEEE Trans Smart Grid 2015;6(6):2669–80. http://dx.doi.org/10.1109/TSG.2015.2453398.
[38] Ma T, Mohammed OA. Economic analysis of real-time large-scale pevs network power flow control algorithm with the consideration of v2g services. IEEE Trans Indus Appl 2014;50(6):4272–80. http://dx.doi.org/10.1109/TIA.2014.2346699.
[39] Zhao Y, An Y, Ai Q, size Research on. Research on size and location of distributed generation with vulnerable node identification in the active distribution network. Transmiss Distrib 2014;8(11):1801–9. http://dx.doi.org/10.1049/iet-gtd.2013.0887.
[40] Baziar A, Kavousi-Fard A. Considering uncertainty in the optimal energy management of renewable micro-grids including storage devices. Renew Energy 2013;59:158–66.
[41] Wu L, Shahidehpour M, Li T. Cost of reliability analysis based on stochastic unit commitment. IEEE Trans Power Syst 2008;23(3):1364–74. http://dx.doi.org/10.1109/TPWRS.2008.922231.
[42] Pourahmadi F, Fotuhi-Firuzabad M, Dehghanian P. Application of game theory in reliability-centered maintenance of electric power systems. IEEE Trans Indus Appl 2017;53(2):936–46. http://dx.doi.org/10.1109/TIA.2016.2639454.
[43] Ruszczyński A, Shapiro A. Stochastic programming models. Handbooks Operat Res Manage Sci 2003;10:1–64.
[44] He Z, Yen GG, Zhang J. Fuzzy-based Pareto optimality for many-objective evolutionary algorithms. IEEE Trans Evol Comput 2014;18(2):269–85. http://dx.doi.org/10.1109/TEVC.2013.2258025.